Transp Porous Med (2011) 88:357–368
DOI 10.1007/s11242-011-9743-8

Effect of Conduction in Bottom Wall on Darcy–Bénard Convection in a Porous Enclosure

H. Saleh · N. H. Saeid · I. Hashim · Z. Mustafa

Received: 12 July 2010 / Accepted: 1 February 2011 / Published online: 19 February 2011

Abstract Conjugate natural convection-conduction heat transfer in a square porous enclosure with a finite-wall thickness is studied numerically in this article. The bottom wall is heated and the upper wall is cooled while the verticals walls are kept adiabatic. The Darcy model is used in the mathematical formulation for the porous layer and the COMSOL Multiphysics software is applied to solve the dimensionless governing equations. The governing parameters considered are the Rayleigh number ($100 \leq Ra \leq 1000$), the wall to porous thermal conductivity ratio ($0.44 \leq K_{\mathrm{r}} \leq 9.90$) and the ratio of wall thickness to its height ($0.02 \leq D \leq 0.4$). The results are presented to show the effect of these parameters on the heat transfer and fluid flow characteristics. It is found that the number of contrarotative cells and the strength circulation of each cell can be controlled by the thickness of the bottom wall, the thermal conductivity ratio and the Rayleigh number. It is also observed that increasing either the Rayleigh number or the thermal conductivity ratio or both, and decreasing the thickness of the bounded wall can increase the average Nusselt number for the porous enclosure.

Keywords Conjugate heat transfer · Natural convection · Porous media · Darcy's law

List of symbols

d, D	Wall thickness, dimensionless wall thickness
g	Gravitational acceleration
K	Permeability of the porous medium

H. Saleh · I. Hashim (✉) · Z. Mustafa
School of Mathematical Sciences, Universiti Kebangsaan Malaysia, UKM,
Bangi, 43600 Selangor, Malaysia
e-mail: ishak_h@ukm.my

H. Saleh
e-mail: twokbi@yahoo.com

N. H. Saeid
Department of Mechanical, Materials and Manufacturing Engineering, The University of Nottingham
Malaysia Campus, 43500 Semenyih, Selangor, Malaysia
e-mail: Nawaf.Saeid@nottingham.edu.my

K_r	Thermal conductivity ratio
k_p	Effective thermal conductivity of porous medium
k_w	Thermal conductivity of wall
L	Width and height of enclosure
$\overline{Nu}$	Average Nusselt number
Ra	Rayleigh number
T	Temperature
u, v	Velocity components in the x- and y-directions
x, y and X, Y	Space coordinates and dimensionless space coordinates

Greek symbols

α	Effective thermal diffusivity
β	Thermal expansion coefficient
ψ, Ψ	Stream function, dimensionless stream function
Θ	Dimensionless temperature
ν	Kinematic viscosity

Subscripts

c	Cold
h	Hot
max	Maximum
p	Porous
w	Wall

1 Introduction

Convective flows within porous materials have occupied the central stage in many fundamental heat transfer analyses and have received considerable attention over the last few decades. This interest is because of its wide range of applications, for example, in high performance insulation for buildings, chemical catalytic reactors, packed sphere beds, grain storage, and such geophysical problems as the frost heave. Porous media are also of interest in relation to the underground spread of pollutants, to solar power collectors, and to geothermal energy systems. Convective flows can develop within these materials if they are subjected to some form of a temperature gradient. Many applications are discussed and reviewed by Ingham and Pop (1998), Pop and Ingham (2001), Ingham et al. (2004), Ingham and Pop (2005), Vafai (2005), and Nield and Bejan (2006).

The convective flows associated with an enclosure heated from below bring about a pattern of convection cells. In each cell, the fluid rotates in a closed orbit and the direction of rotation alternates with successive cells (contrarotative cells). This phenomenon is conventionally referred to in the literature as the Bénard convection. Such a convection phenomenon also receives a broad attention owing to the inherited hydrodynamic fluid stability. The critical Rayleigh number, which signals the onset of natural convection, was first reported by Lapwood (1948) to be equal to $4\pi^2$ for a Darcy fluid flow in a porous medium bounded between two infinite horizontal surfaces maintained at two different isothermal temperatures. This problem is sometimes referred to as the Darcy–Bénard convection. Then 27 years later, Caltagirone (1975) conducted experimental and numerical simulations in 2D and concluded that the Rayleigh number and the aspect ratio are the most important parameters for the

occurrence of the Darcy–Bénard convection. Prasad and Kulacki (1987) studied natural convection in porous media for localized heating from below and found that the heat transfer increases by increasing the length of the heat source. Later, Saeid (2005) extended the work of Prasad and Kulacki (1987) to sinusoidal bottom wall temperature variations. He found that the average Nusselt number increases when the length of the heat source or the amplitude of the temperature variation increases. Bilgen and Mbaye (2001) studied the development of contrarotative cells in fluid-saturated porous enclosures with lateral cooling. They reported in detail the effects of Rayleigh and Biot number on the numbers of contrarotative cells and their circulation modes.

Literatures indicated that most of the reported works on Darcy–Bénard convection do not study the effect of a conductive bottom wall. Applications of conductive bottom wall can be found, for example, in a high-performance insulation for buildings. When the conductivities of the wall and fluid are comparable and the wall thickness is finite, conduction-convection analysis necessary. This coupled conduction-convection problem is known as conjugate convection. Conjugate natural convection in a rectangular porous enclosure surrounded by walls was firstly examined by Chang and Lin (1994a). Their results show that wall conduction effects decrease the overall heat transfer rate from the hot to cold sides of the system. Chang and Lin (1994b) also studied the effect of wall heat conduction on natural convection in an enclosure filled with a non-Darcian porous medium. Baytas et al. (2001) gave a numerical analysis in a square porous enclosure bounded by two horizontal conductive walls. Later, Saeid (2007a) studied conjugate natural convection in a square porous enclosure with two equal-thickness walls. Saeid (2007b) investigated the case when only one vertical wall is of finite thickness. Thermal non-equilibrium model to investigate the conjugate natural convection in porous media was reported by Saeid (2008). Varol et al. (2008) studied a porous enclosure bounded by two solid massive walls from vertical sides at different thicknesses. Al-Amiri et al. (2008) considered the two insulated-horizontal walls of finite thickness and used the Forchheimer–Brinkman-extended Darcy model in the mathematical formulation. Conjugate heat transfer in triangular and trapezoidal porous enclosures were studied by Oztop et al. (2008), Varol et al. (2009a), and Varol et al. (2009b), respectively.

The investigation of the effect of the conductive bottom wall on convective flows in a porous square enclosure has not received much attention. Recent works include those of Varol et al. (2009c) for Darcy–Bénard convection in a triangular porous enclosure and Varol et al. (2010) for a cold water near 4°C in a thick bottom wall enclosure.

The aim of this study is to examine the effect of the conductive bottom wall on Darcy–Bénard convection in a square porous enclosure. This effect on the flow development, temperature distribution, and heat transfer rate in the wall and porous medium will be presented graphically.

2 Mathematical Formulation

A schematic diagram of a porous enclosure with a finite-wall thickness is shown in Fig. 1. The bottom surface of the impermeable wall is heated to a constant temperature T_h, and the top surface of the porous enclosure is cooled to a constant temperature T_c, while the verticals walls are kept adiabatic. In the porous medium, Darcy's law is assumed to hold, the Oberbeck–Boussinesq approximation is used and the fluid and the porous matrix are in local thermal equilibrium.

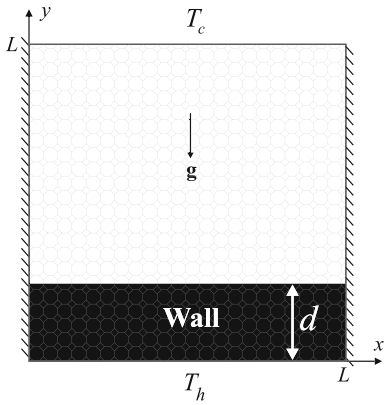

Fig. 1 Schematic representation of the model

With these assumptions, the continuity, Darcy and energy equation for steady, two-dimensional flow in an isotropic and homogeneous porous medium are:

$$\frac{\partial u}{\partial x} + \frac{\partial v}{\partial y} = 0 \tag{1}$$

$$\frac{\partial u}{\partial y} - \frac{\partial v}{\partial v} = -\frac{gK\beta}{\nu}\frac{\partial T_\mathrm{p}}{\partial x} \tag{2}$$

$$u\frac{\partial T_\mathrm{p}}{\partial x} - v\frac{\partial T_\mathrm{p}}{\partial y} = \alpha\left(\frac{\partial^2 T_\mathrm{p}}{\partial x^2} + \frac{\partial^2 T_\mathrm{p}}{\partial y^2}\right) \tag{3}$$

and the energy equation for the impermeable wall is:

$$\frac{\partial^2 T_\mathrm{w}}{\partial x^2} + \frac{\partial^2 T_\mathrm{w}}{\partial y^2} = 0 \tag{4}$$

where the subscripts p and w stand for the porous layer and the wall respectively. No-slip condition is assumed at all the solid-fluid interfaces. The above equations can be written in terms of the stream function ψ defined as $u = \partial\psi/\partial y$ and $v = -\partial\psi/\partial x$. Using the following non-dimensional variables:

$$\begin{aligned} &\Psi = \frac{\psi}{\alpha}, \qquad \Theta_\mathrm{p} = \frac{T_\mathrm{p} - T_\mathrm{c}}{\Delta T}, \qquad \Theta_\mathrm{w} = \frac{T_\mathrm{w} - T_c}{\Delta T}, \\ &X = \frac{x}{L}, \qquad Y = \frac{y}{L}, \qquad D = \frac{d}{L}, \qquad (\text{where } \Delta T = T_\mathrm{h} - T_\mathrm{c} > 0) \end{aligned} \tag{5}$$

the resulting non-dimensional forms of (1–4) are:

$$\frac{\partial^2 \Psi}{\partial X^2} + \frac{\partial^2 \Psi}{\partial Y^2} = -Ra\frac{\partial \Theta_\mathrm{p}}{\partial X} \tag{6}$$

$$\frac{\partial \Psi}{\partial Y}\frac{\partial \Theta_\mathrm{p}}{\partial X} - \frac{\partial \Psi}{\partial X}\frac{\partial \Theta_\mathrm{p}}{\partial Y} = \frac{\partial^2 \Theta_\mathrm{p}}{\partial X^2} + \frac{\partial^2 \Theta_\mathrm{p}}{\partial Y^2} \tag{7}$$

$$\frac{\partial^2 \Theta_\mathrm{w}}{\partial X^2} + \frac{\partial^2 \Theta_\mathrm{w}}{\partial Y^2} = 0 \tag{8}$$

where Ra is the Rayleigh number defined as: $Ra = g\beta K\Delta T L/(\nu\alpha)$. The values of the non-dimensional stream function are zero in the wall region and on the solid-fluid interfaces.

The boundary conditions for the non-dimensional temperatures are:

$$\Theta_w(X,0)=1; \quad \Theta_p(X,1)=0 \tag{9}$$

$$\partial\Theta_p(0,Y)/\partial X=0; \quad \partial\Theta_w(0,Y)/\partial X=0 \tag{10}$$

$$\partial\Theta_p(1,Y)/\partial X=0; \quad \partial\Theta_w(1,Y)/\partial X=0 \tag{11}$$

$$\Theta_p(X,D)=\Theta_w(X,D); \quad \partial\Theta_p(X,D)/\partial Y=K_r\partial\Theta_w(X,D)/\partial Y \tag{12}$$

where $K_r = k_w/k_p$ is the thermal conductivity ratio. The physical quantities of interest in this problem are the average Nusselt number, defined by:

$$\overline{Nu}_w=\int_0^1 \frac{-\partial\Theta_w}{\partial Y}\Big|_{Y=0,D}dY \tag{13}$$

$$\overline{Nu}_p=\int_0^1 \frac{-\partial\Theta_p}{\partial Y}\Big|_{Y=D,1}dY \tag{14}$$

where $\overline{Nu}_w$ represents the dimensionless heat transfer through the walls.

3 Computational Methodology

The governing equations along with the boundary condition are solved numerically by the CFD software package COMSOL Multiphysics. COMSOL Multiphysics (formerly FEMLAB) is a finite-element analysis, solver, and simulation software package for various physics and engineering applications. The authors consider the following application modes in COMSOL Multiphysics. The Poisson's equations mode (poeq) for Eq. 6, the Convection-Conduction equations mode (cc) for Eq. 7 and the conduction equations mode (ht) for Eq. 8.

Several grid sensitivity tests were conducted to determine the sufficiency of the mesh scheme and to insure that the results are grid independent. The authors use the COMSOL Multiphysics default settings for predefined mesh sizes, i.e., extremely coarse, extra coarse, coarser, coarse, normal, fine, finer, extra fine, and extremely fine. In the tests, the authors consider the parameters $D = 0.1$, $K_r = 0.44$, and $Ra = 500$ as tabulated in Table 1. Considering both accuracy and time, a finer-mesh size was selected for all the computations done in this article.

In order to validate the computation code, the previously published problems on Darcy–Bénard convection in a square porous enclosure without conductive bottom wall ($D = 0$) were solved. Table 2 shows that the average Nusselt number and the maximum stream function values are in good agreement with the solutions reported by the literatures. These comprehensive verification efforts demonstrated the robustness and accuracy of this computation.

4 Results and Discussion

The analyses in the undergoing numerical investigation are performed in the following range of the associated dimensionless groups: the wall thickness, $0.02 \le D \le 0.4$; the thermal conductivity ratio, $0.44 \le K_r \le 9.9$; and the Rayleigh number, $100 \le Ra \le 1000$.

Figure 2 illustrates the effects of the wall-thickness parameter D for $Ra = 500$ and $K_r = 0.44$ on the thermal fields and flow fields in the porous enclosure and in the bottom

Table 1 Grid sensitivity check at $D = 0.1$, $K_r = 0.44$, and $Ra = 500$

Predefined mesh size	Mesh elements	$\overline{Nu}_p$	$\overline{Nu}_w$	CPU time (s)
Extremely coarse	74	2.367288	5.262597	0.093
Extra coarse	99	2.382947	5.279511	0.094
Coarser	190	2.365366	5.296369	0.141
Coarse	278	2.356134	5.300857	0.203
Normal	619	2.341694	5.291231	0.344
Fine	942	2.338167	5.29274	0.5
Finer	1984	2.333244	5.29224	0.984
Extra fine	6268	2.32993	5.29197	3.078
Extremely fine	25052	2.328852	5.292062	14.016

Table 2 Comparison of $\overline{Nu}$ and $|\Psi_{max}|$ values with some results from the literature for $D = 0$ (no conductive wall)

Ra	Present		Bilgen and Mbaye (2001)		Caltagirone (1975)	
	$\overline{Nu}$	$\lvert\Psi_{max}\rvert$	$\overline{Nu}$	$\lvert\Psi_{max}\rvert$	$\overline{Nu}$	$\lvert\Psi_{max}\rvert$
50	1.454	2.116	1.443	2.092	1.45	2.112
100	2.654	5.370	2.631	5.359	2.651	5.377
150	3.336	7.379	–	–	–	–
200	3.830	8.941	3.784	8.931	3.813	8.942
250	4.222	10.253	4.167	10.244	4.199	10.253
300	4.549	11.400	4.487	11.394	4.523	11.405

solid wall. As can be seen, the parameter D affects the fluid and the solid temperatures as well as the flow characteristics. The strength of the flow circulation of the fluid-saturated porous medium is much higher for a thin solid bottom wall. The flow circulation breaks up into a perfectly dual contrarotative cells at $D = 0.4$. This is because of the fluid adjacent to the hotter wall has lower density than the the fluid at the middle plane. As a result, the fluid moves upward because of Archimedes force from both the left and right portion of the top wall. When the fluid reaches the upper part of the porous enclosure, it is cooled, so its density increases, then the fluid flows downward at the middle plane of the porous enclosure. This creates a successive cell that is well known as Bénard cells. It is important to note that the Rayleigh number in this study is based on the total height of the enclosure and not on the thickness of the porous layer.

To show the effect of the thermal conductivity ratio K_r on the thermal fields and the circulation of the fluid in the porous enclosure, the isotherms and streamlines are presented in Fig. 3 for $Ra = 500$ and $D = 0.2$. Three different materials are selected: epoxy-water ($K_r = 0.44$); glass-water ($K_r = 2.40$); and epoxy-air ($K_r = 9.90$). It observed that three contrarotative cells are formed as shown in Fig. 3a–c. The clockwise circulation cell refers to natural circulation, i.e., the main cell. As the conductivity ratio increases, the magnitude of the main cell increases while the magnitudes of the secondary (left top) and the third (right bottom) cells decrease and shrink. This phenomenon is because of the temperature gradient near the wall that increases with the increase of the parameter K_r. Thus, much heat transfer

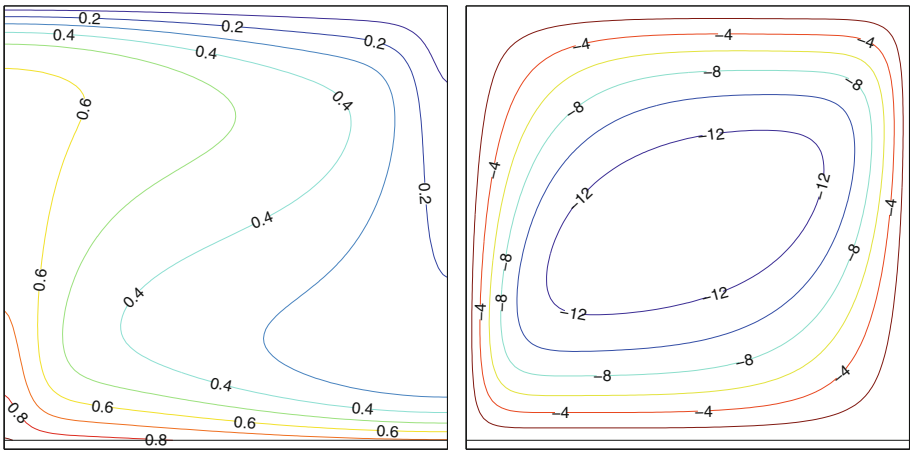

(a) $D = 0.02$

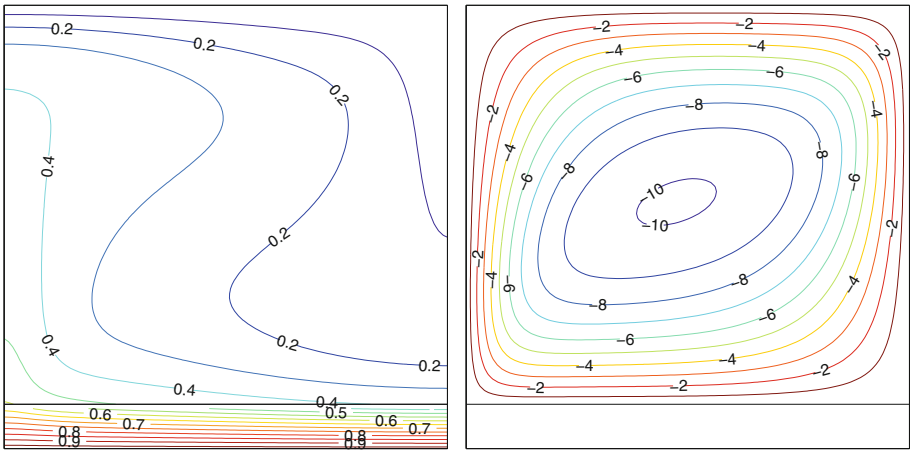

(b) $D = 0.1$

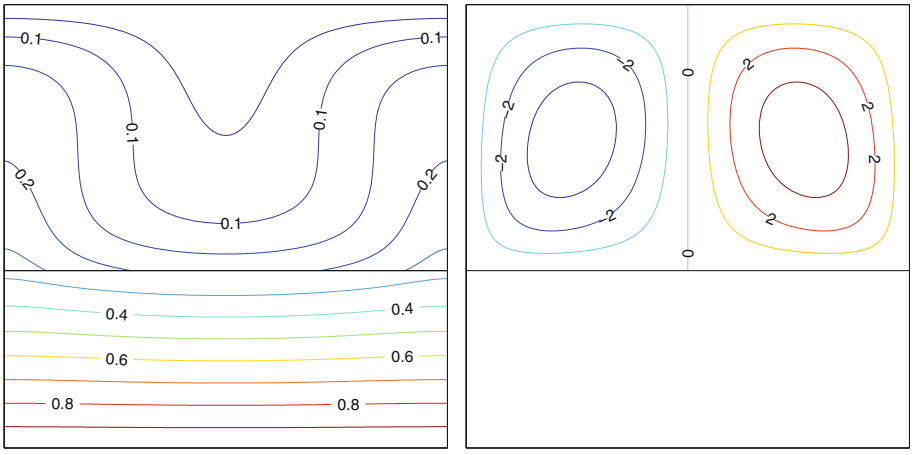

(c) $D = 0.4$

Fig. 2 Isotherms (*left*), streamlines (*right*) at $Ra = 500$ and $K_r = 0.44$

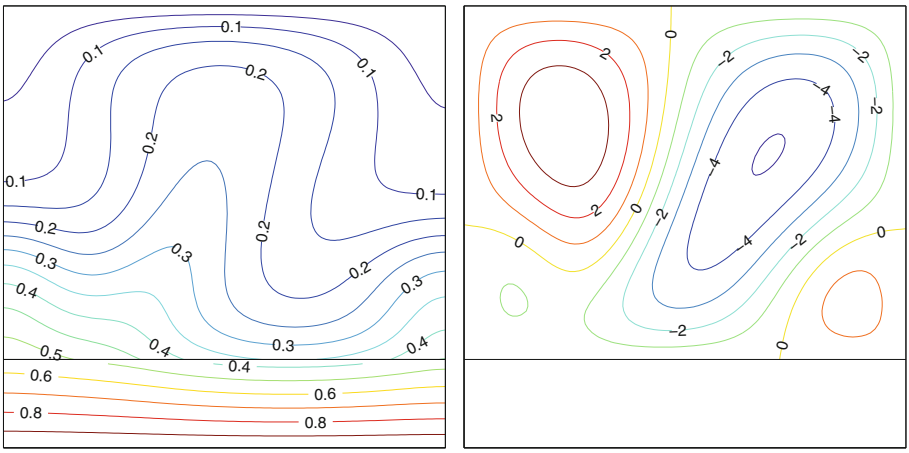

(a) $Kr = 0.44$

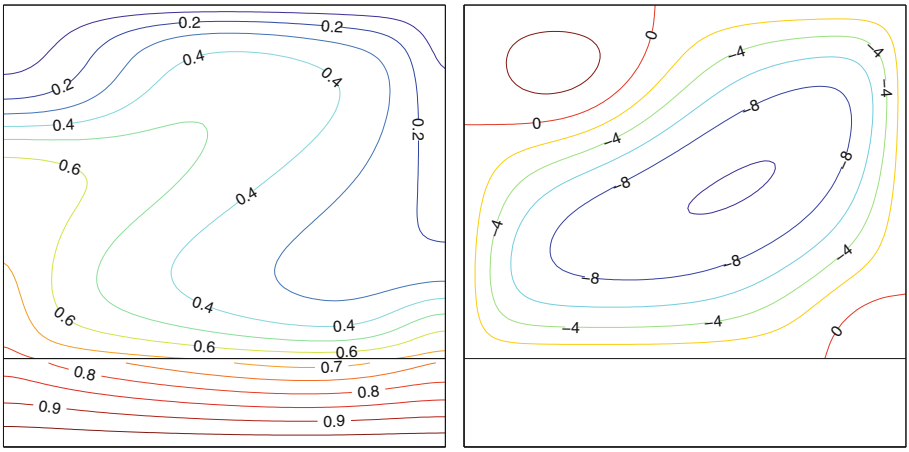

(b) $Kr = 2.40$

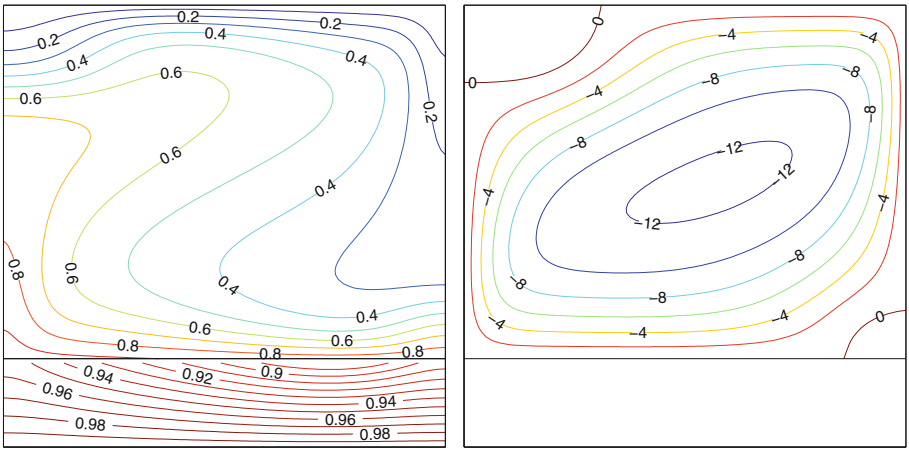

(c) $Kr = 9.90$

Fig. 3 Isotherms (*left*), streamlines (*right*) at $Ra = 500$ and $D = 0.2$

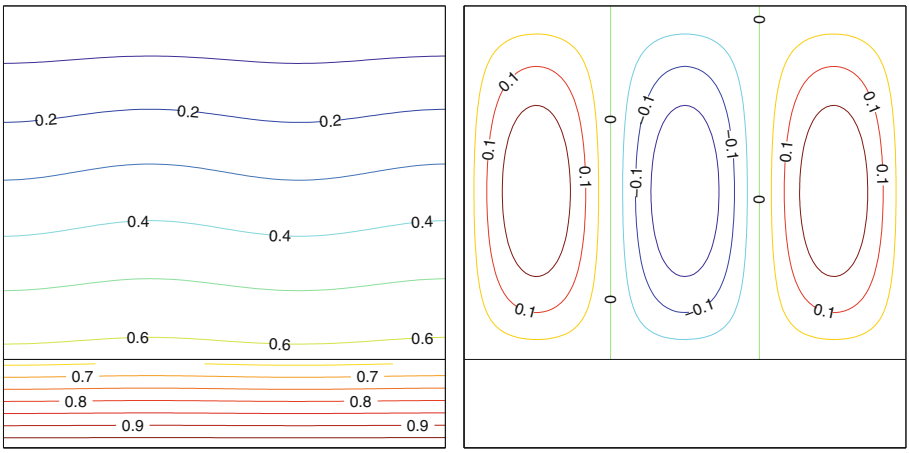

(a) $Ra = 150$

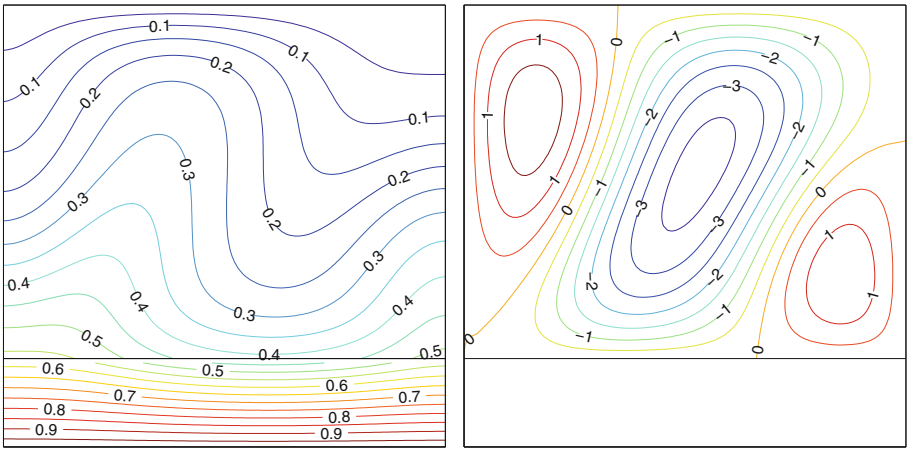

(b) $Ra = 300$

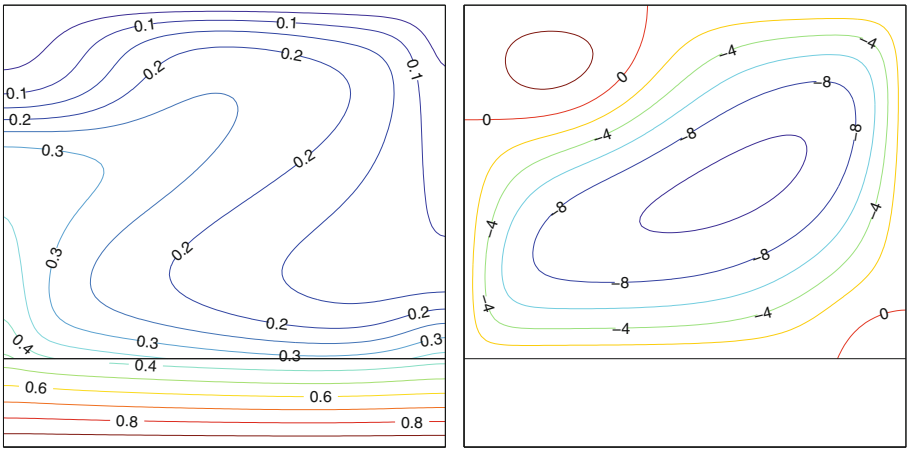

(c) $Ra = 1000$

Fig. 4 Isotherms (*left*), streamlines (*right*) at $K_r = 0.44$ and $D = 0.2$

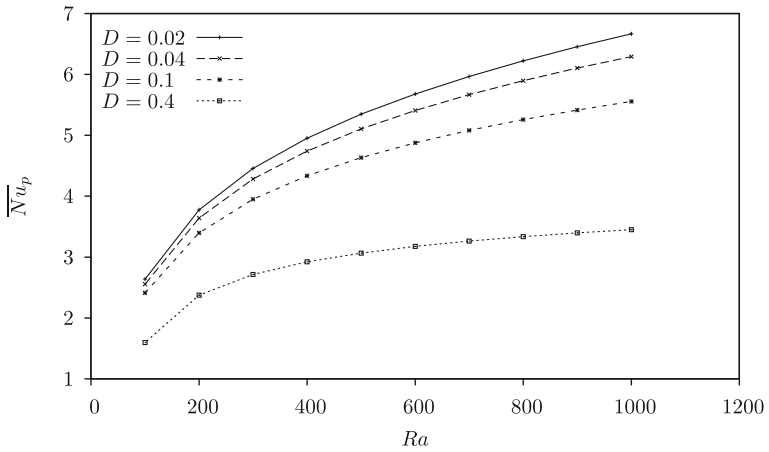

Fig. 5 Variation of $\overline{Nu}_\mathrm{p}$ with Ra for different D

from the bottom solid wall to the porous medium is obtained for higher values of K_r (good conductive solid wall). It is also observed that convection effects inside the porous medium become stronger for higher values of K_r.

Figure. 4a–c shows the effects of Ra on the thermal fields and flow fields in the porous enclosure and in the bottom solid wall with constant values of $K_\mathrm{r} = 0.44$ and $D = 0.2$. As can be seen in Fig. 4a, three contrarotative cells were formed with the same size and strength. When Ra takes higher values as depicted in Fig. 4b and c, the main cell circulation strengthens while the secondary (left) and the third cell weakens and shrinks. Thermal fields show that the temperature distribution is almost uniform in the solid bottom wall for all values of Ra investigated. The thermal fields in the porous enclosure are modified strongly by increasing Ra as shown in Fig. 4b and c. This refers to the strength of convection current related to the Ra values.

Variations of the average Nusselt number with the Rayleigh number are shown in Fig. 5 for different values of the wall thickness D and porous medium made of glass-water ($K_\mathrm{r} = 2.4$). The result presented in Fig. 5 shows that for a thin solid wall, the heat transfer from the fluid increases with increasing Ra. This is because of the increasing of domination of convection heat transfer by increasing the buoyancy force inside the porous medium. Figure. 5 also shows that $\overline{Nu}_\mathrm{p}$ becomes constant for the highest values of the thickness parameter of the solid bottom wall.

Variations of the average Nusselt number with the Rayleigh number are shown in Fig. 6 for different values of K_r with constant $D = 0.1$. Obviously, the heat transfer increases by increasing Ra. The heat transfer enhancement by increasing Ra is more pronounced at higher values of thermal conductivity ratio as shown in Fig. 6. This is because of the temperature gradient near the solid wall that increases with increasing K_r or increasing Ra as shown in Figs. 3 and 4.

Variations of the average Nusselt number with the wall thickness are presented in Fig. 7 for different values of K_r with constant $Ra = 500$. This figure shows that the heat transfer decreases by increasing the solid wall thickness D. There is a considerable difference between the heat transfer for small and large values of K_r. For the epoxy-water material ($K_\mathrm{r} = 0.44$), the heat transfer is almost constant. When K_r takes higher values, heat transfer drops sharply

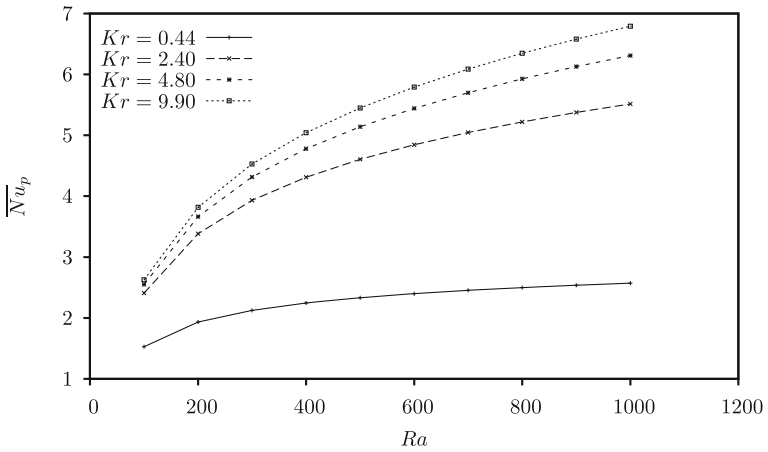

Fig. 6 Variation of $\overline{Nu}_{\mathrm{p}}$ with Ra for different K_{r}

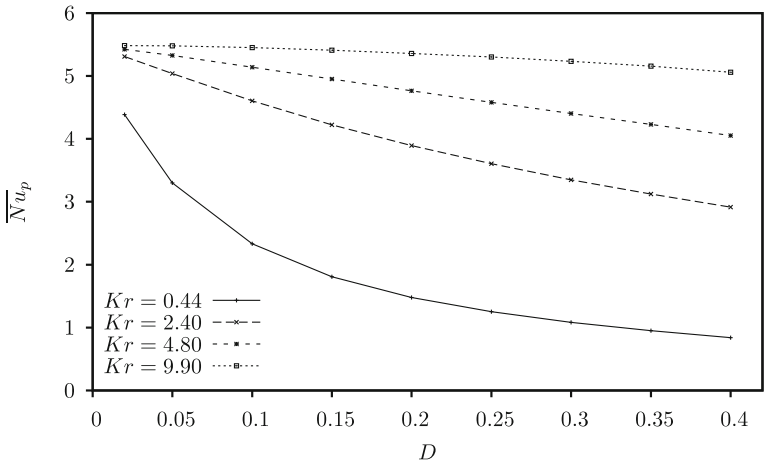

Fig. 7 Variation of $\overline{Nu}_{\mathrm{p}}$ with D for different K_{r}

by increasing D and becomes a conduction mode. This is because of the bottom solid wall that behaves as an insulated material in this case.

5 Conclusions

This numerical simulations study the effects of a conduction in bottom wall on Darcy–Bénard convection in a square porous enclosure. The dimensionless forms of the governing equations are solved using the COMSOL Multiphysics software. Detailed computational results for flow and temperature fields and the heat transfer rates in the enclosure have been presented in graphical forms. The main conclusions of this analysis are as follows:

1. The strength of the flow circulation of the fluid saturated porous medium is much higher with thin walls and/or higher value of the solid to fluid thermal conductivity ratio.

2. The number of contrarotative cells and the strength circulation of each cell can be controlled by the thickness of the bottom wall, the thermal conductivity ratio and the Rayleigh number.
3. The average Nusselt number increases by increasing either the Rayleigh number and/or thermal conductivity ratio, but the average Nusselt number decrease by increasing the wall thickness.

References

Al-Amiri, A., Khanafer, K., Pop, I.: Steady-state conjugate natural convection in a fluid-saturated porous cavity. Int. J. Heat Mass Transf. **51**, 4260–4275 (2008)

Baytas, A. C., Liaqat, A., Grosan, T., Pop, I.: Conjugate natural convection in a square porous cavity. Heat Mass Transf. **37**, 467–473 (2001)

Bilgen, E., Mbaye, M.: Bénard cells in fluid-saturated porous enclosures with lateral cooling. Int. J. Heat Fluid Flow **22**, 561–570 (2001)

Caltagirone, J. P.: Thermoconvective instabilities in a horizontal porous layer. J. Fluid Mech. **72**, 269–287 (1975)

Chang, W. J., Lin, H. C.: Natural convection in a finite wall rectangular cavity filled with an anisotropic porous medium. Int. J. Heat Mass Transf. **37**, 303–312 (1994a)

Chang, W. J., Lin, H. C.: Wall heat conduction effect on natural convection in an enclosure filled with a non-darcian porous medium. Numer. Heat Transf. A **25**, 671–684 (1994b)

Ingham, D. B., Pop, I.: Transport phenomena in porous media. Elsevier Science, Oxford (1998)

Ingham, D. B., Bejan, A., Mamut, E., Pop, I.: Emerging technologies and techniques in porous media. Kluwer, Dordrecht (2004)

Ingham, D. B., Pop, I.: Transport phenomena in porous media III. Elsevier Science, Oxford (2005)

Lapwood, E. R.: Convection of a fluid in a porous medium. In: Proc. Camb. Philos. Soc. **44**, 508–521 (1948)

Nield, D. A., Bejan, A.: Convection in Porous Media, 3rd ed. Springer, New York (2006)

Oztop, H. F., Varol, Y., Pop, I.: Effects of wall conduction on natural convection in a porous triangular enclosure. Acta Mech. **200**, 155–165 (2008)

Pop, I., Ingham, D. B.: Convective Heat Transfer: Mathematical and Computational Modelling of Viscous Fluids and Porous Media. Pergamon, Oxford (2001)

Prasad, V., Kulacki, F. A.: Natural convection in horizontal porous layers with localized heating from below. J. Heat Transf. **109**, 795–798 (1987)

Saeid, N. H.: Natural convection in porous cavity with sinusoidal bottom wall temperature variation. Int. Comm. Heat Mass Transf. **32**, 454–463 (2005)

Saeid, N. H.: Conjugate natural convection in a vertical porous layer sandwiched by finite thickness walls. Int. Comm. Heat Mass Transf. **34**, 210–216 (2007a)

Saeid, N. H.: Conjugate natural convection in a porous enclosure: effect of conduction in one of the vertical walls. Int. J. Thermal Sci. **46**, 531–539 (2007b)

Saeid, N. H.: Conjugate natural convection in a porous enclosure sandwiched by finite walls under thermal nonequilibrium conditions. J. Porous Media **11**, 259–275 (2008)

Vafai, K. (ed.): Handbook of Porous Media, 2nd edn. Taylor and Francis, New York (2005)

Varol, Y., Oztop, H. F., Koca, A.: Entropy generation due to conjugate natural convection in enclosures bounded by vertical solid walls with different thicknesses. Int. Comm. Heat Mass Transf. **35**, 648–656 (2008)

Varol, Y., Oztop, H. F., Pop, I.: Conduction-natural convection in a partitioned triangular enclosure filled with fluid saturated porous media. J. Porous Media **12**, 593–611 (2009a)

Varol, Y., Oztop, H. F., Pop, I.: Entropy analysis due to conjugate-buoyant flow in a right-angle trapezoidal enclosure filled with a porous medium bounded by a solid vertical wall. Int. J. Thermal Sci. **48**, 1161–1175 (2009b)

Varol, Y., Oztop, H. F., Pop, I.: Conjugate heat transfer in porous triangular enclosures with thick bottom wall. Int. J. Numer. Meth. Heat Fluid Flow **19**, 650–664 (2009c)

Varol, Y., Oztop, H. F., Mobedi, M., Pop, I.: Visualization of heat flow using Bejan's heatline due to natural convection of water near 4° C in thick walled porous cavity. Int. J. Heat Mass Transf. **53**, 1691–1698 (2010)